Lead Article

Acta Cryst. (1991). A47, 297-313

Zeolite Crystallography. Structure Determination in the Absence of Conventional Single-Crystal Data*

By Lynne B. McCusker

Institute of Crystallography, ETH, Zurich, Switzerland

(*Received 29 October 1990; accepted 7 February 1991*)

Abstract

Zeolite molecular sieves are a class of aluminosilicates whose technologically important properties are intimately related to their structures. Since most synthetic zeolites are only available as powders and not as single crystals, conventional crystallographic techniques cannot be used to solve their structures. The crystallographic difficulties are exacerbated by the pseudosymmetry, faulting, disorder and impurity problems, which are relatively common in zeolite materials. Over the years, zeolite crystallographers have developed a number of approaches to these problems and these are discussed. The techniques include informed model building, various computer approaches to model generation, application of direct methods to powder data, microcrystalline diffraction and exploitation of magic angle spinning NMR and electron microscopy. Usually a number of methods are combined to construct a framework structure model and to test it for feasibility. Once a reasonable model has been produced, Rietveld refinement will not only confirm (or reject) the framework proposal but also reveal further details of the structure. Although the techniques described were developed for application to zeolite structures, many can probably be applied to other systems.

Introduction

Zeolites are used as ion exchangers (*e.g.* in detergents to replace phosphates and in nuclear waste treatment to remove radioactive Cs^+ and Sr^+ ions), as drying agents (*e.g.* in chemical laboratories and between the panes in double-glazed windows), as molecular sieves (*e.g.* for separating branched from straight-chain hydrocarbons or *para-* from *meta*-xylene), as shape-selective acid catalysts (*e.g.* in the cracking and reforming of oil and in the synthesis of fine chemicals) and even as chicken- and pig-feed additives. This diverse and complex chemistry is intimately related to the structures of these materials and that makes zeolite crystallography an especially rich and rewarding field of research.

Unfortunately, it also means that no single paper can cover the whole spectrum of zeolite structural science. There is a vast crystallographic literature on zeolite single-crystal structure determinations, on the various ion-exchanged forms of zeolites, on the location of organic 'templates' within zeolite frameworks, on the location of sorbed molecules in zeolitic channels, on the transformation of one zeolite framework to another, on the changes occurring in a zeolite framework during catalysis and on the determination of new zeolite framework structures in the absence of conventional single-crystal data. It is the latter aspect of zeolite crystallography I have decided to concentrate on in this paper. This rather narrowly defined area is a tremendously fertile one, and one that I hope will be of interest to crystallographers outside the field of zeolites as well as to those within. A number of the techniques developed for zeolite framework structure determination can certainly be applied to other systems.

A brief introduction to zeolites and the crystallographic difficulties they pose will be followed by a description of several methods of framework structure determination, some samples of the type of information that can be gleaned from subsequent Rietveld refinement and a discussion of some relatively new structural characterization techniques [magic angle spinning (MAS) NMR and microcrystal diffraction] now being applied to zeolitic systems.

Zeolites and zeolite-like materials

Classically, zeolites are defined as a class of crystalline aluminosilicates with (i) a relatively rigid anionic aluminosilicate framework with well defined channels

---

* *Editorial note*: This invited paper is one of a series of comprehensive Lead Articles which the Editors invite from time to time on subjects considered to be timely for such treatment.

0108-7673/91/040297-17$03.00

and cavities; (ii) mobile exchangeable cations (usually group 1 or 2) which balance the negative charge of the framework; and (iii) water which can be removed by heating or evacuating without affecting the framework topology (Breck, 1974; Seff, 1976). More recently this definition has been relaxed somewhat to encompass a larger class of related microporous materials. With this expanded description, any three-dimensional framework structure with tetrahedrally coordinated atoms (T atoms) joined to one another through oxygen bridges and with a framework density less than 21 T atoms/1000 Å^3 can be considered zeolite like (Meier & Olson, 1987). Thus, some pure silica materials, the aluminophosphate-based molecular sieves, some beryllophosphates and some structures with cavities but no channels (clathrasils) can be included in discussions of zeolite structures. For the purposes of this paper, I will use this wider definition, since the crystallographic problems found in all these materials are similar.

For a more comprehensive introduction to the field of zeolites, the reader is referred to the book *Zeolite Molecular Sieves* by Breck (1974). Although this book is more than 15 years old, it was written by one of the pioneers in the field and still provides an excellent introduction to the subject. The textbook *Introduction to Zeolite Science and Practice*, which was used for the Zeist Summer School preceding the International Zeolite Association (IZA) conference in Amsterdam in 1989, will be published shortly, and should include some of the newer aspects of zeolite science (van Bekkum, Flanigen & Jansen, 1991). Overviews of various developments since 1974 can also be found in the Conference Proceedings of the IZA (Meier & Uytterhoeven, 1973; Katzer & Gould, 1977; Rees, 1980; Olson & Bisio, 1984; Murakami, Iijima & Ward, 1986; Jacobs & van Santen, 1989).

Nomenclature

For the non-zeolite scientist, a few words about zeolite nomenclature are probably in order. The Structure Commission of the International Zeolite Association is responsible for assigning three-letter codes to each new framework topology as it is established. At the moment there are 75 codes approved and five under consideration. These codes denote only the connectivity of the tetrahedral atoms in the highest possible space group. Chemical composition, unit-cell size and the observed symmetry of the type of material are not used. Some representative framework topologies are shown in Fig. 1. In the text, relevant three-letter codes are indicated in boldface type.

Since hundreds of zeolitic materials, some naturally occurring and some synthesized in the laboratory, are known, the classification by structure type proves to be extremely useful. It is not unusual to encounter a

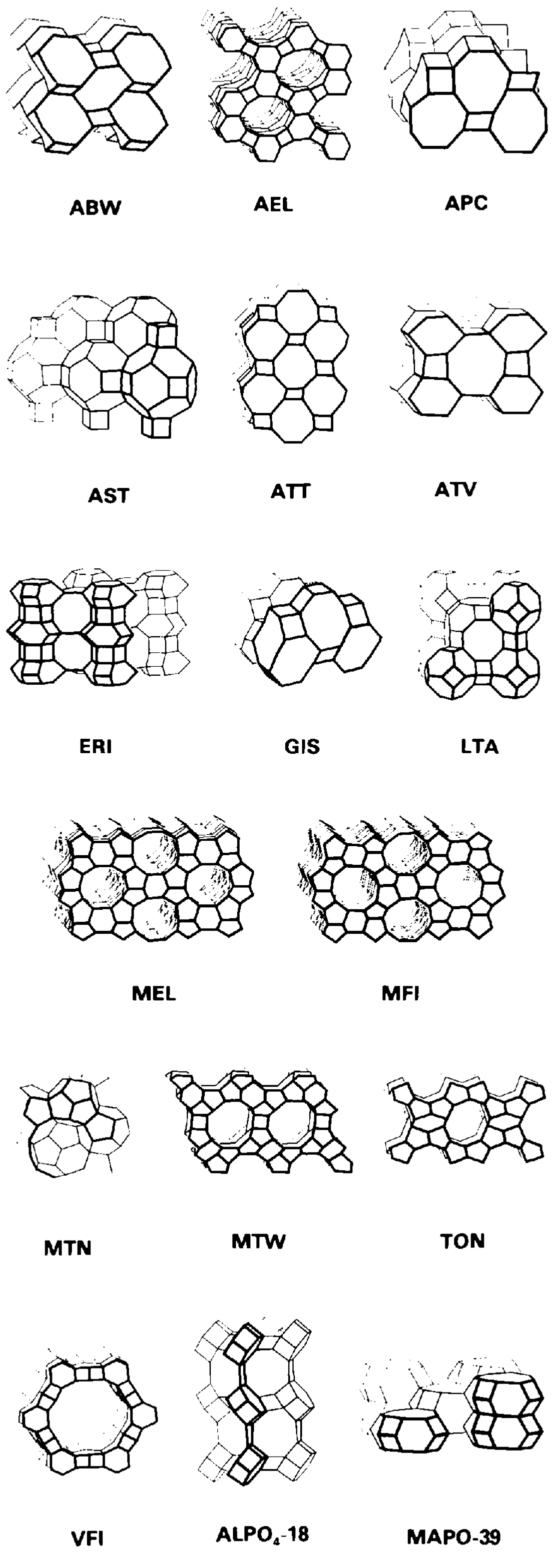

Fig. 1. Some examples of zeolite framework topologies. Each node represents a T atom. For clarity, oxygen bridges have been omitted and rings with fewer than ten T atoms have been made opaque. Additional framework topologies are shown in Figs. 3, 4, 5 and 9.

number of different names for materials which have the same framework topology. Sometimes different names indicate real differences in chemical composition or symmetry, but often they are simply names assigned by different laboratories to very similar materials. An extreme example is that of the 21 zeolite and zeolite-like materials with the **MFI** topology (AMS-1B, AZ-1, BOR-C, boralite C, encilite, FZ-1, LZ-105, NU-4, NU-5, silicate, silicalite 1, TS-1, TSZ, TSZ-III, TZ-01, USC-4, USI-108, ZBH, ZKQ-1B, ZMQ-TB and ZSM-5) and a more typical one is that of the ten with the **GIS** topology (the minerals amicite, garronite, gismondine, gismondite and gobbinsite and the synthetic materials MAPSO-43, Na-P1, Na-P2, synthetic zeolite B and synthetic zeolite P).

Three reference handbooks, which contain detailed information on each of the structure types [*Atlas of Zeolite Structure Types* (Meier & Olson, 1987), *Compilation of Extra-Framework Sites in Zeolites* (Mortier, 1982) and *Collection of Simulated XRD Powder Patterns for Zeolites* (von Ballmoos & Higgins, 1990)], are published under the auspices of the Structure Commission and are updated periodically in rotation.

Quite often the term *n*-ring will be used to describe a channel opening, a cation site, or some other feature of the framework structure. A 6-ring, for example, is a ring containing six *T* atoms and six O atoms. A cation is often located near the center of a 6-ring, where it can coordinate to three of the six O atoms. Similarly, an 8-ring is a small channel opening, a 10-ring a medium one and a 12-ring a large one.

A channel system can be one-, two- or three-dimensional, depending upon the nature of the intersection of the channels. For example, the structure type **AEL** has a one-dimensional channel system with 10-ring pore openings, **APC** a two-dimensional one with 8-ring pore openings and **FAU** a three-dimensional one with 12-ring pore openings. A zeolite can also have more than one channel system. For example, zeolite rho (**RHO**) has two non-intersecting three-dimensional channel systems (Fig. 2).

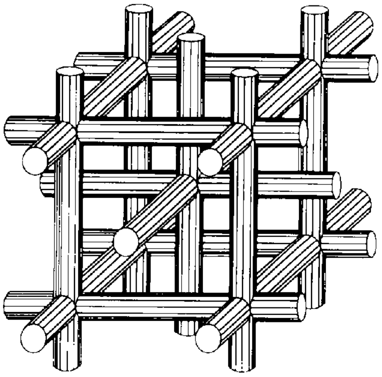

Fig. 2. The two non-intersecting three-dimensional channel systems of zeolite rho (**RHO**). See Fig. 3 for the framework topology.

A zeolite has to be calcined at elevated temperatures (usually in air) to remove water and organic material from the channels before it can be used as a sorbent, a molecular sieve or a catalyst. In general, diffraction data on the calcined material is preferred over that on the as-synthesized form for framework structure determination studies, since the non-framework material tends to complicate the problem. However, symmetry or crystallinity considerations can make an investigation of the as-synthesized form preferable.

Crystallographic difficulties

The chemical composition of the tetrahedral atoms and the type and number of cation sites available in a given framework structure determine that zeolite's ion-exchange properties, the size and shape of the channels and the dimensionality of the channel system govern its molecular sieving properties, and the location of the acid sites in the channels and cavities control its catalytic applications. Consequently, knowledge of the structure is of paramount importance to a zeolite scientist. Unfortunately, very few synthetic zeolitic materials are available as single crystals suitable for structure analysis, so various strategies have been developed over the years to overcome this problem. It is these novel, and often ingenious, methods of framework structure determination which will form the basis of this paper.

Beyond the fact that most zeolites are only available as polycrystalline powders, a number of crystallographic problems are inherent to zeolite structure analysis and these must be borne in mind. For example, the high symmetry of the framework structure is rarely obeyed by non-framework species and this leads to partial occupancies and disordered structures and/or to pseudosymmetry problems. There are almost as many examples as there are zeolite structure refinements: *e.g.* the location of the tetrapropylammonium ion in ZSM-5 (Baerlocher, 1984; van Koningsveld, Jansen & van Bekkum, 1987), the arrangement of Ag^+ ions in zeolite A (Kim & Seff, 1978; Gellens, Mortier & Uytterhoeven, 1981), or the location of acetylene sorbed in Mn^{2+} and Co^{2+} forms of zeolite A (Riley & Seff, 1975).

Furthermore, the cations and sorbed molecules can cause subtle distortions of the framework which lead to changes in symmetry that are difficult to see in a powder diffraction pattern. For example, the zeolite rho (**RHO**) unit cell contracts significantly upon dehydration, but no change in systematic absences or crystal system is apparent. In fact, refinement shows that the space group changes from $Im\bar{3}m$ to $I\bar{4}3m$ and that a considerable tetrahedral distortion occurs (Fig. 3) (McCusker & Baerlocher, 1984; Parise, Gier, Corbin & Cox, 1984). The high-silica zeolite ZSM-5 (**MFI**) crystallizes in space group *Pnma*

($a = 20{\cdot}1$, $b = 19{\cdot}9$, $c = 13{\cdot}4$ Å), becomes monoclinic ($P2_1/n$) when calcined and cooled to room temperature (van Koningsveld, Jansen & van Bekkum, 1990) and reverts to orthorhombic upon heating or upon sorption of *p*-xylene (van Koningsveld, Tuinstra, van Bekkum & Jansen, 1989). However, the space group of the *p*-xylene sorption complex is not *Pnma* as one might expect but $P2_12_12_1$. Such subtle differences are almost impossible to determine from systematic absences in powder data.

The tetrahedral atoms are sometimes ordered, but since the differences in the X-ray scattering factors for Al, Si and P, the most common tetrahedral atoms, are so small, such ordering is often difficult to detect, and even more difficult to refine. Neutron scattering cross sections are slightly better, but still far from ideal. The Si and Al atoms in zeolite A (**LTA**) alternate throughout the structure and thereby reduce the symmetry from $Pm\bar{3}m$ to $Fm\bar{3}c$. Yet, even with this extremely strict ordering, the most intense reflection arising from the superlattice (531) has only 10% of the intensity of the more intense ones arising from the pseudo-cell (Gramlich & Meier, 1971). In most cases, where strict ordering (such as that in zeolite A or in aluminophosphates) is not apparent, average *T*-atom scattering factors are calculated and only average *T*-atom positions refined. Even in structures with well ordered *T* atoms, pseudosymmetry problems often arise in the refinement.

Stacking faults are not uncommon in zeolites. A subset of the zeolite framework topologies can be described in terms of stacking of 6-rings in a manner analogous to the closest packing of spheres. These zeolites are particularly prone to stacking faults and all the attendant problems. For example, the framework of ZK-14, a synthetic chabasite (**CHA**), can be described as an *AABBCC* stacking of 6-rings (Fig. 4). Its powder diffraction pattern shows broadening of the reflections with $l \neq 3n$, its electron diffraction patterns show streaking parallel to **c*** and the high-resolution electron diffraction image shows the stacking faults themselves (Cartlidge, Wessicken & Nissen, 1983).

A more extreme problem in this direction is that of intergrowths in which two phases are intimately mixed on a submicrometer scale. The first in-depth investigation of this phenomenon was an electron diffraction study of erionite/offretite (**ERI**/**OFF**) intergrowths, which have the 6-ring stacking sequences *AABAAC* and *AAB*, respectively (Bennett & Gard, 1967). Since then, several zeolites exhibiting similar behavior have been examined.

Only recently has ZSM-11 (**MEL**) been synthesized without ZSM-5 (**MFI**) intergrowths (Fyfe, Gies, Kokotailo, Pasztor, Strobl & Cox, 1989). The same type of layer is found in both materials, but those in ZSM-5 are related to one another by an inversion center (*i*-type stacking), while those in ZSM-11 are related by a mirror plane (σ-type stacking). A statistical model for calculating the diffraction pattern for various ratios of the two (a more complicated procedure than a simple algebraic addition of the two diffraction patterns) was introduced by Perego, Cesari & Allegra (1984). They assumed a random Bernoullian distribution of stacking faults and a fault probability parameter *p* and derived the equation

$$I_{hkl}(s) = \frac{N}{U}\,\frac{2\bar{L}_{hkl}}{1+(2\pi\bar{L}_{\text{instr}}s)^2}\,|\bar{F}(hkl)|^2, \qquad (1)$$

where *N* is the number of diffracting unit cells, *U* is the unit-cell volume, $\bar{L}_{hkl}$ is the effective average crystal thickness with respect to the *hkl* vector, $(2\pi\bar{L}_{\text{instr}})^{-1}$ describes the instrumental broadening and

$$|\bar{F}_{hkl}|^2 = 1/2[P(F_AF_A^* + F_BF_B^*) + Q(F_AF_B^* + F_BF_A^*)]/AB, \qquad (2)$$

where *A*, *B*, *P* and *Q* are functions of the fault probability parameter *p*, F_A is the structure factor for the subcell of ZSM-5 and F_B is the structure factor

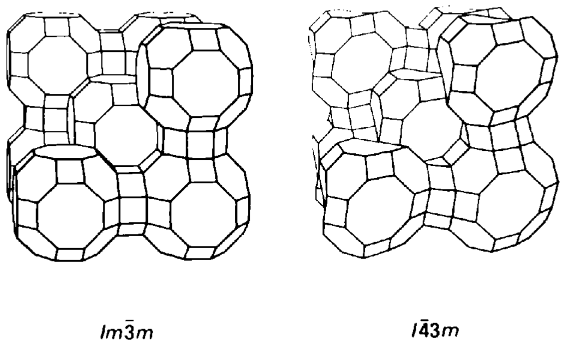
$Im\bar{3}m$ $I\bar{4}3m$

Fig. 3. The zeolite rho (**RHO**) framework structure in two different space groups. The zeolite crystallizes in $Im\bar{3}m$, but distorts to $I\bar{4}3m$ upon calcination.

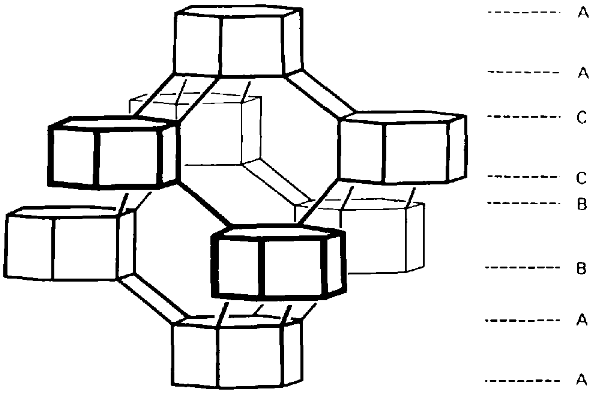

Fig. 4. The **CHA** framework topology showing the *AABBCC* stacking of 6-rings. Each node represents a *T* atom. Oxygen bridges have been left out for clarity.

for the subcell of ZSM-11. Using this approach, they were able to model the increasing broadness of the $h+k+l=2n+1$ reflections with increasing probability of σ-type stacking and to estimate the relative percentages of ZSM-5 and ZSM-11 in a sample by fitting the calculated powder pattern to the experimental one.

The synthetic zeolite ZSM-20 is an intergrowth of a face-centered-cubic arrangement of sodalite cages (*ABC* stacking) joined through double 6-rings (**FAU**) and its hexagonal analog (*ABAB* stacking) (Fig. 5). In this case, it is the hexagonal form that is difficult to synthesize in pure form, although that has now been accomplished (Delprato *et al.*, 1989). Treacy, Newsam & Deem (1989) have apparently developed a much simpler general algorithm based on the recursive properties of faulting for simulating the diffraction patterns of such highly faulted materials.

Perhaps the most extreme example of intergrowth in the field of zeolites is that of the technologically important zeolite beta. The elucidation of the framework structure was reported simultaneously by two groups (Newsam, Treacy, Koetsier & de Gruyter, 1988; Higgins *et al.*, 1988). These papers describe one of the most impressive pieces of detective work in the zeolite literature. The tetragonal layer, which is characteristic of zeolite beta, can be rotated clockwise or counterclockwise with respect to the previous layer (Fig. 6) and a long-range order of stacking has not yet been reported. Apparently the energy difference between the two alternatives is minimal and the result is disorder along the *c* axis. The theoretical end members are enantiomers (with 4_1 or 4_3 screw axes), so zeolite beta has the intriguing potential of having a chiral framework structure (if an ordered structure can be synthesized) coupled with a large pore channel system. A further interesting aspect of this structure is the fact that no matter how the layers are stacked, a three-dimensional 12-ring channel system is formed. Consequently, zeolite beta is of considerable importance for catalytic applications. The only other zeolite structures with three-dimensional large-pore channel systems are the hexagonal version of **FAU** mentioned above, which is expensive to make, and **FAU** itself, which is the topology of zeolite Y, the active component of the fluid cracking catalyst (FCC) used by the oil industry for cracking and reforming processes.

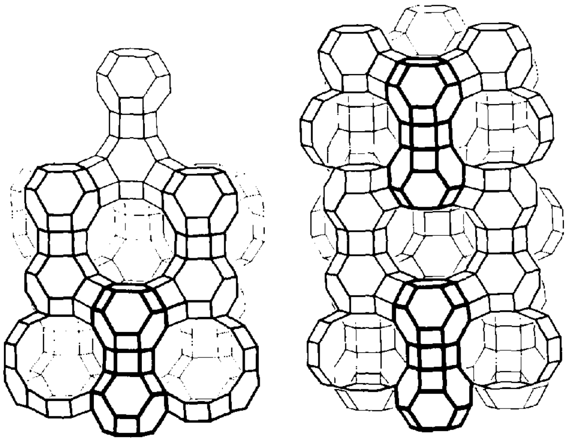

(*a*) (*b*)

Fig. 5. The two stackings of sodalite cages found intergrown in the zeolite ZSM-20: (*a*) the face-centered cubic *ABC* stacking (**FAU**) and (*b*) the hexagonal *ABAB* stacking.

Twinning is not an uncommon feature of zeolite crystals, but it does not usually interfere with powder work. It can even be an asset in reducing preferred-orientation problems. However, in extreme cases, it can cause confusion in the indexing and symmetry determination process. For many years it was believed that there were both cubic and tetragonal versions of the synthetic zeolite P ($a=b\sim c\sim 10$ Å). This was based on the observed powder diffraction patterns. In fact, a series of ion-exchange experiments followed by structure refinement showed the 'cubic' P to be highly twinned tetragonal P (**GIS**) (Baerlocher & Meier, 1970, 1972).

Finally, there is the matter of sample quality. The synthesis of pure highly crystalline zeolite materials is an art requiring patience and persistence. The synthesis conditions required to produce different framework topologies are often very similar and, as a result, multiple phase and/or poorly crystalline samples are not uncommon. Time spent in the optimization of synthesis conditions is never wasted from the crystallographer's point of view. The additional information provided by a good powder diffraction pattern can mean the difference between solving and not solving a structure.

Framework structure determination

Model building

The first six zeolite framework structure analyses (**ANA**, **CAN**, **NAT**, **SOD**, **EDI** and **THO**) were done in the 1930's (Taylor, 1930; Pauling, 1930*a*, *b*; Taylor & Jackson, 1933; Taylor, Meek & Jackson, 1933). At that time, Patterson maps, direct methods and even computers were unknown. The scientists solved the structures of these natural zeolites by combining chemical, geometric, symmetry and single-crystal diffracted intensity information with logic. Sixty years later we have many more techniques available to us and, although these are fully exploited, the most common method of zeolite structure determination remains one of model building based on data from various sources.

The structures of many of the natural zeolites were investigated during the 1930's, 1950's and 1960's. These were single-crystal structure determinations and will not be dealt with in detail here. However, those structures provided the basic geometric and structural data used by later crystallographers to construct zeolite framework structure models.

In the 1950's and 1960's, the characterization of new zeolitic materials usually included (i) the chemical composition, (ii) the density, (iii) the unit-cell dimensions from powder diffraction, (iv) symmetry information from electron diffraction and (v) pore size from sorption experiments. By combining such data with the expected *T*-O distances, O-*T*-O and *T*-O-*T* angles (from related structures), crystallographers were able to solve several of the early synthetic zeolite structures.

A simple example is that of zeolite A (**LTA**), whose structure was reported in 1956 (Breck, Eversole, Milton, Reed & Thomas, 1956). The unit-cell composition, derived from chemical analysis, density and unit-cell-size data, was found to be $Na_{12}[(AlO_2)_{12}(SiO_2)_{12}].27H_2O$; sorption experiments showed that the zeolite has a 5 Å pore opening, which is indicative of an 8-ring channel; the powder diffraction pattern could be indexed on a primitive cubic unit cell with $a = 12{\cdot}32$ Å; and no systematic absences were observed. The highest possible space group, $Pm\bar{3}m$, was assumed. With this symmetry, a general position has a multiplicity of 48, so the 24 *T* atoms per unit cell had to possess at least mirror symmetry. Furthermore, because of size and symmetry considerations, an 8-ring could be placed in only a very limited number of positions within the unit cell. The structure was solved by putting a flat 8-ring on each of the faces of the cube and connecting them to one another across the corners (Fig. 7). Subsequent investigations showed the Si and Al to be ordered and the true unit-cell parameter to be twice as long (Gramlich & Meier, 1971), but the proposed framework topology is correct.

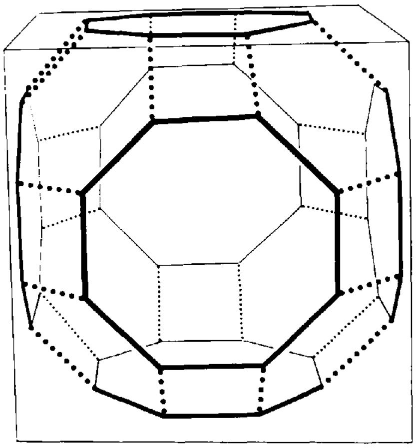

Fig. 7. The structure solution of zeolite A (**LTA**). Flat 8-rings centered on each face of the 12·3 Å cube can be joined to one another as shown to form the large cage of zeolite A.

More recent examples of structure solution by model building are much more complicated, but the principles are the same. Probably the most complex zeolite structure solved in this manner is that of ZSM-5 (**MFI**) with 12 *T* atoms in the asymmetric unit (Kokotailo, Lawton, Olson & Meier, 1978; Olson, Kokotailo, Lawton & Meier, 1981). In that investigation, very small single crystals (20 × 30 × 40 μm) were available, so limited single-crystal data could be used to check the symmetry and to generate low-quality Patterson maps and direct-methods solutions. Although structure solution was not possible on the basis of the X-ray data alone, the Patterson maps proved to be useful in the model-building process. A parallel investigation on silicalite, which also has the **MFI** framework topology, yielded the same result using similar methods and data from a twinned crystal (Flanigen *et al.*, 1978).

A series of structures, including (among others) theta-1 (**TON**) with four *T* atoms in the asymmetric unit (Highcock, Smith & Wood, 1985), EU-1 (**EUO**) with ten (Briscoe, Johnson, Shannon, Kokotailo & McCusker, 1988) and $AlPO_4$-31 with two (Bennett & Kirchner, 1990), has also been solved in the last few years by model building. For **TON**, the symmetry was established with electron diffraction and then the results of a series of two-dimensional Fourier projections generated from 11 strong peaks in the powder pattern were used as a basis for structure modeling. In the case of **EUO**, electron diffraction techniques also played a key role in determining the space group and unit-cell parameters. The *C*-centered orthorhombic lattice parameters suggested a pseudo-hexagonal arrangement of 12-rings and the systematic absences a glide plane perpendicular to that plane. Model building progressed from there. For $AlPO_4$-31 only cell dimension, symmetry, sorption and density information were used to construct the model.

Model testing

Once a model has been created, it must be evaluated. First, it must conform to the observed symmetry and approximate unit-cell size, have the appropriate pore openings and be consistent with any other information available. If these rudimentary requirements are met, the geometry of the model can be optimized for the observed symmetry and unit-cell dimensions. This is usually done by distance least-squares (DLS) refinement (Meier & Villiger, 1969), where the atomic coordinates are adjusted to give ideal *T*-O distances and O-*T*-O and *T*-O-*T* angles. Hill & Gibbs (1979) performed a statistical analysis of the correlation between *T*-O distances and *T*-O-*T* angles for silica polymorphs, silicates, aluminates and phosphates and found, as expected from semi-empirical MO calculations, a $-\sec\angle TOT$ dependence of the *T*-O

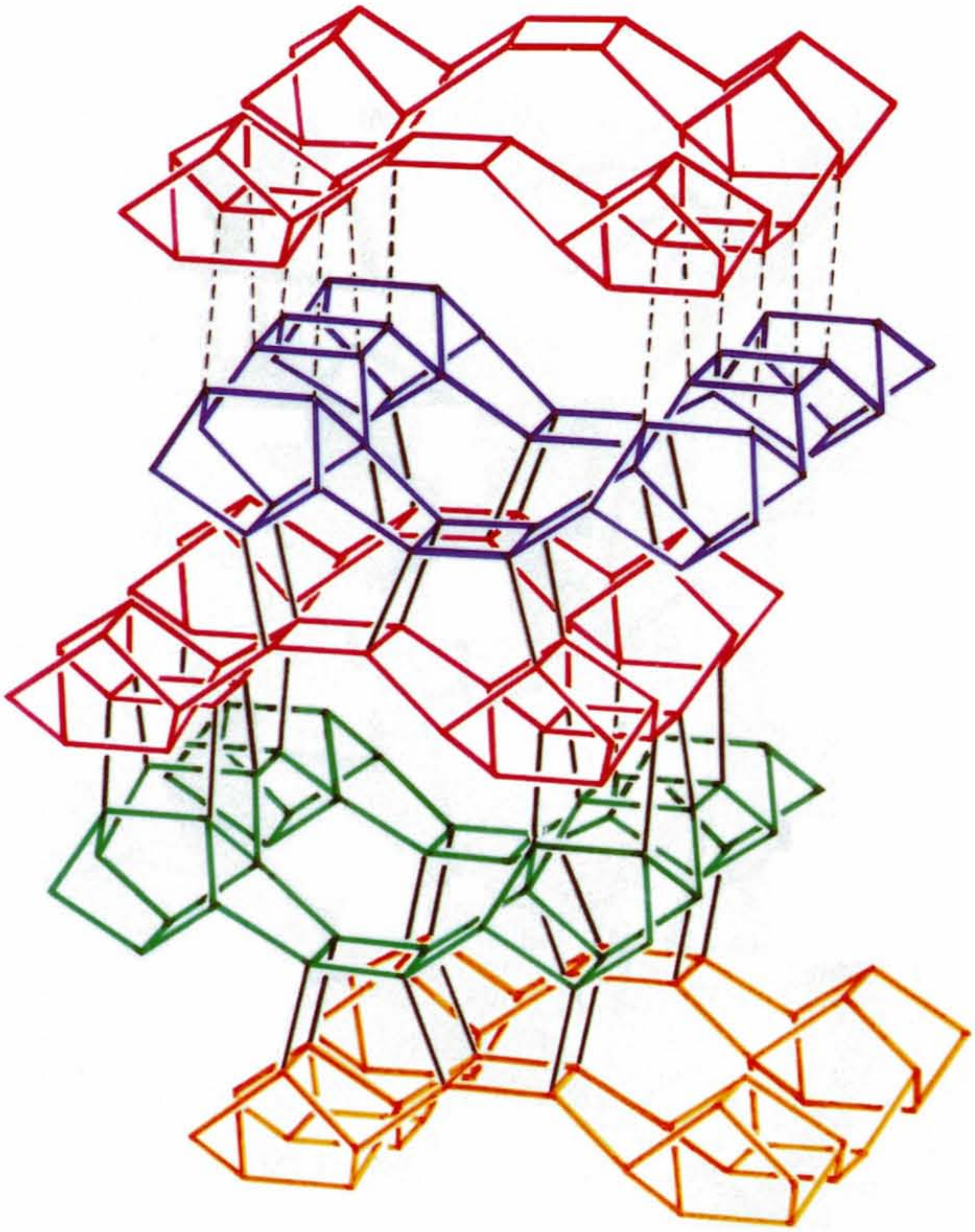

Fig. 6. A possible stacking of the tetragonal layer characteristic of the zeolite beta. The first four layers (orange, green, red, blue) are related by a 4_1 axis and form one of the theoretical end-member structures of zeolite beta. The fifth layer, however, is rotated in the 4_3 sense with respect to the fourth layer. Instead of the first (orange) layer being repeated, the third (red) layer is generated and an intergrowth structure is formed.

distance. This information can also be used in the geometry optimization process.

In a DLS refinement, the residual function in (3) below is minimized with respect to the atomic coordinates (and the unit-cell parameters, if desired) in a least-squares procedure.

$$R = \sum_j w_j^2 [D_j^{\text{pre}} - D_j^{\text{calc}}]^2. \qquad (3)$$

D_j^{pre} is the prescribed distance between two atoms (from related structures), D_j^{calc} the calculated distance (from the model) and w_j the weight for that distance (usually the reciprocal of the estimated standard deviation for the prescribed distance). The current version of the original program is *DLS*-76 (Baerlocher, Hepp & Meier, 1977). To facilitate the creation of a *DLS*-76 input file, Bialek (1991) has written the pre-*DLS* program *KRIBER*. Distance least-squares refinement is a remarkably successful empirical approach to computer modeling of zeolite framework structures (Catlow & Cormack, 1987). The much more costly and time-consuming energy-minimization techniques are unnecessary for model testing.

If a framework model cannot be optimized for the observed symmetry and unit-cell dimensions, the structure proposal is unlikely to be correct and many models can be eliminated in this way. Furthermore, if the choice of space group is in doubt, *DLS* refinement can sometimes indicate which is(are) the more probable one(s).

Once geometry-optimized atomic coordinates have been determined, it is a simple matter to calculate the powder diffraction pattern for that model. The two best-known programs for doing this are *POWD*10 (Smith, Nichols & Zolensky, 1983) and *LAZY PULVERIX* (Yvon, Jeitschko & Parthé, 1977). The pattern can then be compared with the experimentally observed one. An exact match of the patterns cannot be expected, but significant similarity should be apparent if the model is correct. If the sample has not been calcined before the diffraction pattern is measured, the intensities at low angles are likely to be too high in the calculated pattern. Also the presence of heavy cations like K^+ can have a significant influence on the lower-angle reflection intensities.

This procedure of geometry optimization followed by powder-pattern generation is applicable whenever a model structure is to be evaluated.

Hypothetical structures

Most laboratories involved in zeolite structure analysis have a set of hypothetical structures. These are usually the models that were produced and subsequently discarded in the course of a structure analysis. There is always a hope that the material corresponding to such a structure will be prepared and that the work of building the model, optimizing the geometry and generating a powder pattern will not be wasted. Some groups, on the other hand, have taken the approach of generating series of hypothetical structures systematically. An excellent review of the concepts used to produce such series is given by Smith (1988). The limiting factor in this approach to structure solution is that an infinite number of three-dimensional four-connected framework topolgies can be generated and sensible constraints, which have yet to be found and defined, need to be included to reduce the number to manageable proportions. Certainly there is potential in this direction, and a Consortium for Theoretical Frameworks under the direction of Professor J. V. Smith has been established at the University of Chicago to organize a database of hypothetical zeolite structures.

Bennett–Schomaker method

Several automated or semi-automated approaches to zeolite framework structure solution have been devised. The first of these is the Bennett–Schomaker method (Bennett, 1988). The appropriate number of *T* atoms are placed in a unit cell with the observed dimensions and symmetry and are systematically moved through the asymmetric unit. *T–T* distances of approximately 3 Å which form a three-dimensional four-connected net are sought. This is obviously a very time-consuming process, but then again, so is model building. The program prevents *T* atoms from getting too close to mirror planes (*i.e.* not actually on the mirror plane but less than 1·5 Å from it). Unfortunately, at the moment the method is limited by time requirements to a small number of *T* atoms per asymmetric unit. Nonetheless, it was used to solve the structure of the aluminophosphate molecular sieve $AlPO_4$-16 (**AST**) (Bennett & Kirchner, 1991).

Brunner method

The second such method is one devised by G. O. Brunner and is based on a survey of the known zeolite structures. His observation that the largest voids in zeolite framework structures usually occur at points of highest symmetry can be used to generate hypothetical structures (Brunner, 1990). The points of high symmetry and those incompatible with tetrahedral geometry (*e.g.* $\bar{1}$ or $2/m$) are treated as centers of repulsion and the positions of the randomly distributed *T* atoms are then refined according to the calculated forces. At a later stage, additional forces between *T* atoms are introduced to promote the formation of appropriate *T–T* distances. The method has been tested on several known zeolite framework structures and was used to generate the framework topology of MAPO-39 (McCusker, Brunner & Ojo, 1990) before its structure had been established.

In his survey, Brunner also noted that while the fragment consisting of two 4-rings sharing a common edge occurred in 22 zeolite framework structures, only

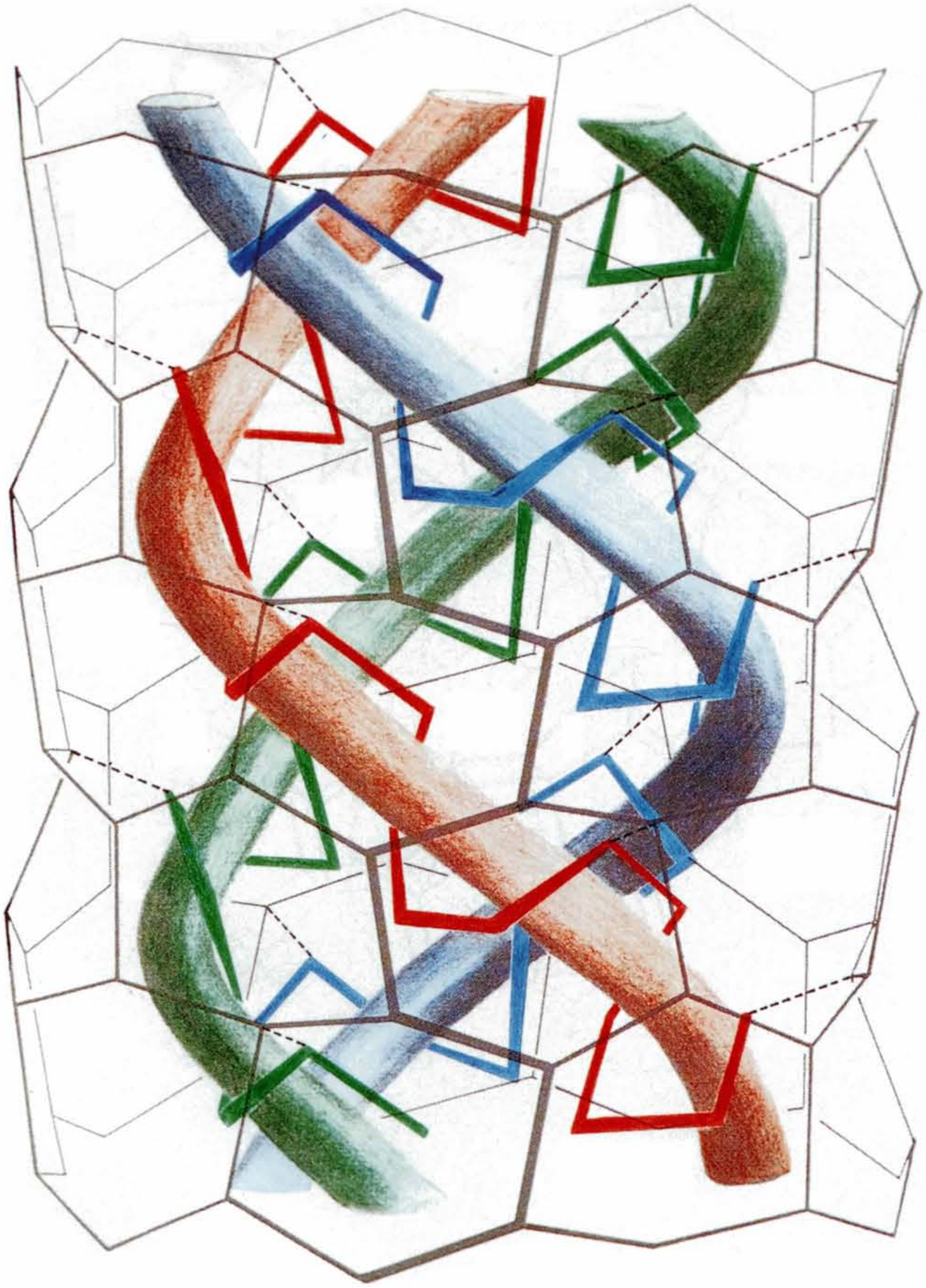

Fig. 10. The triple helix of water molecules (connected by colored bonds) within the 18-ring channel of VPI-5 (**VFI**). Framework O atoms have been left out for clarity. The general form of each strand of the helix has been drawn in to assist the eye and to show the spiral formed by the water along the main direction of the helix. The three symmetry-equivalent strands of the helix have been drawn in three different colors to reduce confusion. Bonds to framework Al atoms are indicated by dashed lines.

the *cis* conformation of this fragment was observed. Such empirical observations based on data from known structures can be very useful in the evaluation of the plausibility of hypothetical structures and it is likely that additional observations of this kind still remain to be found and exploited. The aluminophosphate VPI-5 (**VFI**) proved to be an exception to the above rule, but there the Al atom between the two 4-rings is coordinated to two H_2O molecules in addition to the four framework O atoms - *i.e.* it is octahedrally not tetrahedrally coordinated. Thus, the chemical composition of the framework is an important factor in the evaluation process.

Simulated annealing

The last of these methods for generating plausible framework models is that of simulated annealing, which was introduced by Deem & Newsam (1989). In a way this is a combination of the two previously described methods. As in the Bennett-Schomaker method, the appropriate number of T atoms are placed (arbitrarily in this case) in a unit cell with the observed dimensions and the appropriate symmetry constraints. An 'energy' function based on T-T distances, T-T-T angles and the number of first-nearest neighbors is then minimized by optimizing the coordinates of the T atoms. This optimization is accomplished by Monte Carlo methods using simulated annealing. The 'energy' curves as a function of T-T distance and of T-T-T angle are derived from data from known zeolite structures (and hence the similarity to the Bunner method). A zeolite with an unknown structure (which was later shown to have the **ABW** topology) was investigated using simulated annealing. Two runs produced 20 trial structures which proved to represent three different topologies. The correct topology was then determined by comparing the observed diffraction pattern with the three simulated ones. As in the Bennett-Schomaker method, there is a limitation on the number of T atoms that can be handled comfortably. The authors suggest that more restrictive 'energy' functions are required for the more complicated structures (those with more than six unique T atoms).

Direct methods using powder data

The obvious question arises as to the feasibility of applying crystallographic techniques to zeolite framework structure determination. Given that only polycrystalline material is available, how far can one get using the conventional methods of structure solution? This question has been addressed by a number of groups, including some in the zeolite field. The major stumbling block is the extraction of individual reflection intensities from the X-ray or neutron powder diffraction pattern. Once that has been accomplished, single-crystal techniques can be employed. Only the positions of the T atoms need be determined, since coordinates for the bridging O atoms can be calculated from them. Difference Fourier maps based on the framework structure can then be generated to reveal the location of non-framework species.

Experience in the application of direct methods to powder data has led to the formulation of a few guidelines. The extraction of reflection intensities from the powder pattern is critical. Most groups use the program *ALLHKL* (Pawley, 1981), but new improved programs are being developed (Jansen, Peschar & Schenk, 1990; Baerlocher, 1990). The treatment of exactly or partially overlapping reflections needs to be improved and several groups are working in this direction. The work in progress includes (i) examination of triplets, quartets and even quintets involving both overlapping and non-overlapping reflections to get a probability function for the relative intensities of overlapping reflections (Jansen *et al.*, 1990; Cascarano, Favia & Giacovazzo, 1990), and (ii) a maximum-entropy-based approach involving the improvement of a Patterson function followed by back transformation (Gramlich, 1988). It is essential to include all reflections, whether they overlap with others or not and whether they have high or low intensity. A simple-minded equipartition of the intensity for overlapping reflections is better than leaving the reflections out and it should not be forgotten that a low-intensity reflection contains just as much information as does a high intensity one.

The problem of overlapping reflections cannot be overemphasized, but it can be minimized experimentally by collecting data with the highest possible resolution. This is usually accomplished by using one of the synchrotron facilities with a high-resolution powder diffractometer [SRS, Daresbury (Pattison, Cernik & Clark, 1989), HASYLAB, Hamburg (Arnold *et al.*, 1989) or NSLS, Brookhaven, NY (Cox, Hastings, Cardoso & Finger, 1986)], but careful alignment and judicious use of slits with a conventional in-house diffractometer can yield surprisingly good results.

In Table 1, data are presented for silicalite (**MFI**), with 12 T atoms in the asymmetric unit, and for sigma-2 (**SGT**), with four, to illustrate the difficulties encountered in the extraction of reflection intensities and the subsequent application of direct methods to more complex zeolite structures. Plots of comparable sections of data collected on each of these materials and the respective *ALLHKL* refinements (integrated intensity extraction) are shown in Fig. 8. Positions of symmetry-allowed reflections have been indicated along the 2θ axes. These plots indicate immediately the difference in the complexity of the two problems. The data were collected using similar wavelengths at comparable synchrotron-radiation facilities. Silicalite has lower symmetry and a larger unit cell and, con-

Table 1. *Extracted intensity data for silicalite and sigma*-2

	Silicalite	Sigma-2
Synchrotron facility	SRS	NSLS
Wavelength (Å)	1·4963	1·5468
Range (°2θ)	7–40	8·5–73
Step size (°2θ)	0·01	0·01
FWHM range (°2θ)	0·045–0·059	0·037–0·077
Space group	$Pnma$	$I4_1/amd$
a (Å)	20·062	10·238
b (Å)	19·910	10·238
c (Å)	13·414	34·382
Reflections:		
Total	287	258
Severely overlapping (within 0·15 FWHM of another reflection)	58	26
$\|F\| > 2{\cdot}0\sigma(F)$	57	174
$\|F\| > 1{\cdot}5\sigma(F)$	72	190
$\|F\| > 1{\cdot}0\sigma(F)$	87	211
T atoms/asymmetric unit	12	4

sequently, a higher concentration of reflections in any given 2θ range. Intensities were extracted for a similar number of reflections from the powder patterns of the two materials. If one subtracts those reflections within 0·15 of a FWHM (full width at half maximum) of one another (these are considered to be severely overlapping), there are still 229 for silicalite and 232 for sigma-2. However, the reliability of the intensities is markedly lower for silicalite. At the 2σ level, only 57 of the reflections are observed (*vs* 174 for sigma-2). The vast majority of the reflections are below the 1σ level. The fact that almost all reflections in the pattern are partially overlapping seriously reduces the certainty with which the intensities can be determined and this has obvious consequences regarding the application of direct methods.

In evaluating the feasibility of solving a zeolite framework structure by direct methods using only powder diffraction data, one can calculate the number of T atoms in the unit cell from the unit-cell size, the chemical composition and the density. Then, considering the likely symmetries, one can estimate the number of T-atom sites in the asymmetric unit by assuming they will occupy as many general positions as possible. This number is a minimum, but the data in Table 2 show that this estimate is often close to the number actually found. A rule of thumb is that if there are at least ten reflections with $|F| > 2\sigma(F)$ for each T atom in the asymmetric unit, direct methods have a reasonable chance of producing useful results (not necessarily the complete structure). A list of several zeolites with their symmetries, the number of T atoms in the asymmetric unit estimated from the assumed space group, the number of T atoms actually found and their unit-cell volumes is given in Table 2. The advantage of using a higher space group and thereby reducing the complexity of the problem is clear (*e.g.* **GIS** or $AlPO_4$-18 in Table 2). Small deviations from a higher space group can often be ignored in the initial stages of structure solution where the establishment of the connectivity of the T atoms is of prime importance. Refinement of the structure can then be done in the correct space group.

The structure of $LiAlSiO_4.D_2O$ (**ABW**) with two T atoms in the asymmetric unit was determined by direct methods from three different sets of data (X-ray powder diffractometer, Guinier photograph and neutron powder diffractometer) (Norby, Christensen & Anderson, 1986). With the X-ray diffractometer data, two T atoms, two O atoms and two spurious peaks were found; with the Guinier data, the two T atoms were located; and with the neutron data, one T atom, five O atoms and one D atom were found. Although the problem was a small one and the framework structure a known one, this work demonstrates very nicely the potential of the method, its applicability to both neutron and X-ray data and the complementarity of neutron and X-ray data.

The structure of $AlPO_4$-12-TAMU (**ATT**) was also solved by direct methods using powder diffraction data obtained with a conventional X-ray source (Rudolf, Saldarriaga-Molina & Clearfield, 1986). This was a particularly difficult problem because the space group, $P2_12_12$, is non-centrosymmetric. Nonetheless, after some initial difficulties, the authors were able to locate all six T atoms in the E map generated with 120 reflections (half of which were not observed). A series of difference Fourier maps was then generated to locate the remaining atoms.

The structure of sigma-2 (**SGT**), a clathrasil with an unknown framework, was determined completely *ab initio* from high-resolution synchrotron powder data (McCusker, 1988). The best direct-methods solution gave the positions of all four T atoms and four of the seven O atoms in the asymmetric unit (Fig. 9) and the first difference Fourier map showed the remaining three O-atom positions very clearly. Subsequent refinement coupled with Fourier syntheses revealed the location of the partially disordered 1-aminoadamantane in the large cage. Although this structure is of only average complexity, the fact that eight correct positions were found among the 12 highest peaks in the E map is very encouraging and bodes well for the more complex zeolite structures. It also demonstrates the advantage of using high-resolution data.

The framework structure of the aluminophosphate molecular sieve $AlPO_4$-18 was solved by model building based on fragments gleaned from direct-methods solutions (Simmen, McCusker, Baerlocher & Meier, 1991). A distorted 8-ring approximately perpendicular to **b** and a row of three edge-sharing 4-rings with a less-obvious orientation were found in several of the E maps generated and that information was exploited in the model-building process. This structure solution also highlights a positive aspect of pseudosymmetry. The powder pattern of the calcined material could be indexed on an orthorhombic unit cell (*Cmcm*), although the true symmetry, which describes the strict alternation of Al and P, is monoclinic (*C*2/*c*). By treating the two types of *T* atoms as equivalent in the first approximation, the determination of the framework structure was reduced from a six to a three *T*-atom problem. Rietveld refinement was then performed in the correct space group.

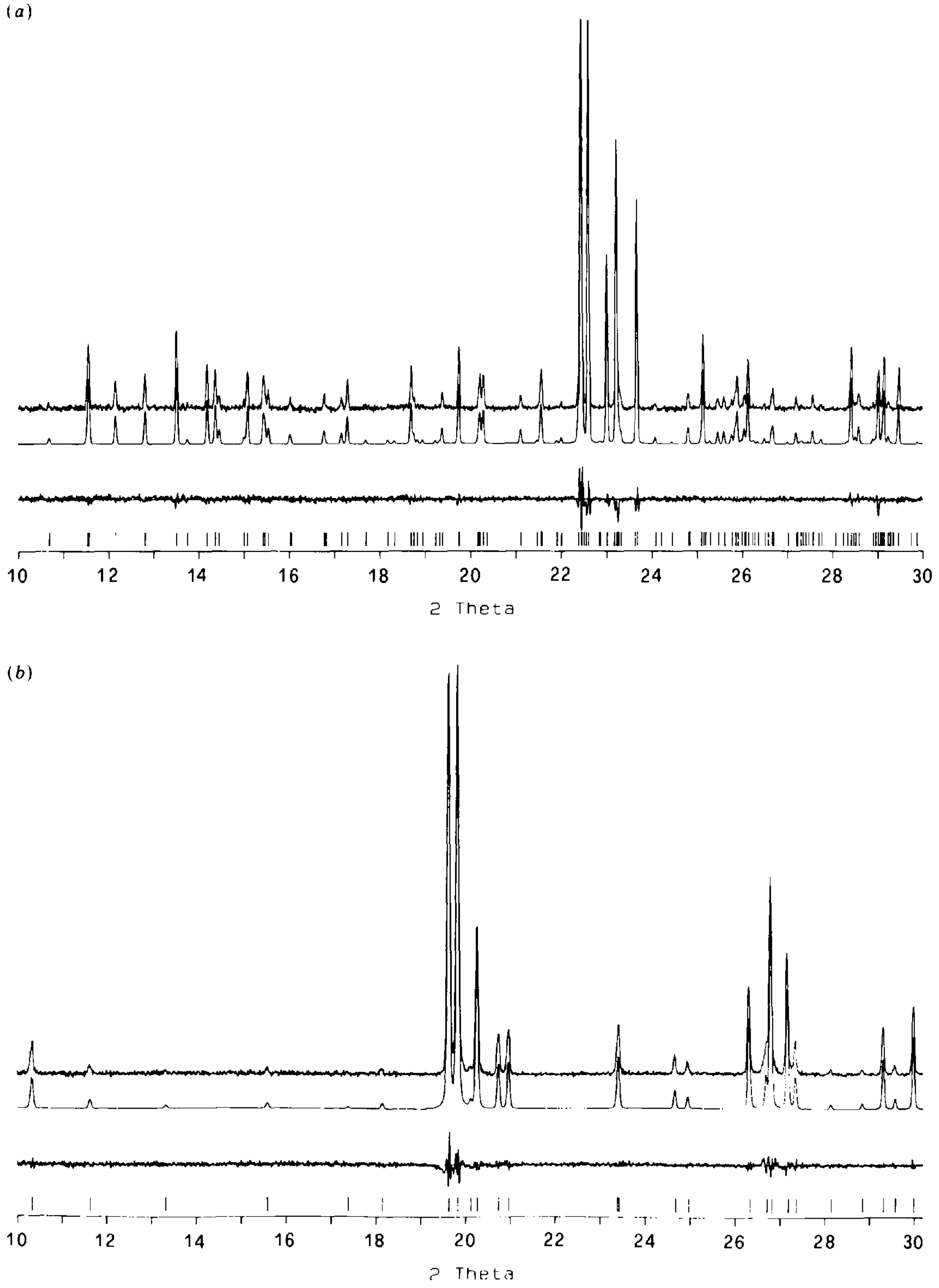

Fig. 8. Sections of the observed (top), calculated (middle) and difference (bottom) profiles from the *ALLHKL* refinement (integrated intensity extraction) of (*a*) silicalite and (*b*) sigma-2. The 2θ positions of symmetry-allowed reflections are indicated along the bottom of each plot.

Table 2. *Some zeolite framework topologies and their symmetries*

Zeolite	Space group (order)	T atoms per unit cell	T atoms in asymmetric unit		Cell volume (Å^3)
			Estimated	Observed	
ABW	$Imma$ (16)	8	1	1	422
	$Pna2_1$ (8)	8	1	2	422
AST	$Fm\bar{3}m$ (192)	40	2	2	2406
	$F23$ (48)	40	2	4	2406
ATT	$Pmma$ (8)	12	2	2	714
	$P2_12_12$ (4)	24	6	6	1429
EUO	$Cmma$ (16)	112	7	10	6170
FAU	$Fd\bar{3}m$ (192)	192	1	1	15 678
FER	$Immm$ (16)	36	3	4	2030
GIS	$I4_1/amd$ (32)	16	1	1	1013
	$P2_1/c$ (4)	16	4	4	1013
LEV	$R\bar{3}m$ (36)	54	2	2	3546
LTA	$Pm\bar{3}m$ (48)	24	1	1	1861
	$Fm\bar{3}c$ (192)	192	1	2	14 888
MEL	$I\bar{4}m2$ (8)	96	6	7	5414
MFI	$Pnma$ (8)	96	12	12	5360
MOR	$Cmcm$ (16)	48	3	4	2783
NON	$Fmmm$ (32)	88	4	5	4559
OFF	$P\bar{6}m2$ (12)	18	2	2	1160
SGT	$I4_1/amd$ (32)	64	2	4	3605
TON	$Cmc2_1$ (8)	24	3	4	1201
$AlPO_4$-18	$Cmcm$ (16)	48	3	3	3130
	$C2/c$ (8)	48	6	6	3130
MAPO-39	$I4/mmm$ (32)	16	1	1	887

Rietveld refinement

In the previous section, a number of methods used to generate a reasonable model for a new zeolite framework structure were discussed. It must be understood that the production of such a model is not a structure determination, it is the creation of a feasible structure proposal. A comparison of the powder diffraction pattern generated from the geometry-optimized atomic coordinates of the model with the experimentally observed pattern will only indicate whether or not a model is likely to be correct. If a projection of the model corresponds to one in the actual structure, but the third dimension is wrong, the calculated pattern will have many features in common with the experimental one. Only a successful refinement will show definitively whether or not a proposed model is correct.

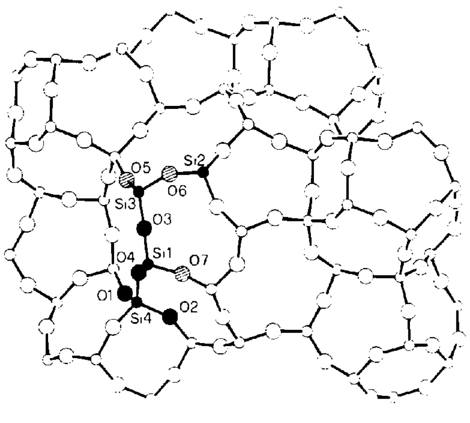

Fig. 9. The sigma-2 (**SGT**) framework structure showing the atoms found in the direct-methods solution (filled circles) and those found in the first difference Fourier map (striped).

A recent example of this fact is provided by the structure of $AlPO_4$-25 (**ATV**) (Richardson, Smith & Pluth, 1990), which is the calcination product of $AlPO_4$-21. The framework structure of $AlPO_4$-21 contains both four- and five-coordinate Al atoms and it was suggested that the structure of $AlPO_4$-25 may well have the same connectivity, but with all the Al atoms tetrahedral (*i.e.* with the Al–O–Al bridge eliminated). The powder diffraction pattern generated from this model resembled that of $AlPO_4$-25, and the proposed model was considered to be very likely (in fact, a three-letter code was assigned to it by the Structure Commission). It was not until a refinement was attempted a year later that the correct structure emerged. The two models have a projection in common, but the linkage between the layers differs significantly.

Consequently, a structure determination cannot be considered complete until the model has been refined satisfactorily with the measured diffraction data. Since the materials under discussion here are polycrystalline, the preferred method is Rietveld (whole pattern) refinement. For more information on this subject, the reader is referred to the *Proceedings of the Rietveld Analysis Workshop* organized recently by the IUCr Commission on Powder Diffraction (Young, 1991). Rietveld refinement of a framework structure model usually produces much more than just confirmation or rejection of a proposed topology. Details of symmetry and of framework geometry and/or the location of non-framework atoms are also extracted in the process.

Since framework models are frequently generated in the highest possible space group, refinement is also necessary to establish the correct symmetry. Rietveld refinement of the ZSM-12 structure (**MTW**) using synchrotron data (Fyfe, Gies, Kokotailo, Marler & Cox, 1990) revealed the true symmetry to be $C2/c$ with $a = 24{\cdot}86$, $b = 5{\cdot}01$, $c = 24{\cdot}33$ Å and $\beta = 107{\cdot}7°$ although the topological symmetry is $C2/m$ with $c = 12{\cdot}15$ Å. The role ^{29}Si MAS NMR played in this space-group determination is discussed in the next section.

Similarly, the structure of the aluminophosphate VPI-5 (**VFI**) was found to have an unexpectedly low symmetry (McCusker, Baerlocher, Jahn & Bülow, 1991). The topological space group is $P6_3/mcm$ and, if strict alternation of Al and P is assumed, it is reduced to $P6_3cm$. In fact, the correct space group proved to be $P6_3$. In this refinement, not only was the proposed framework structure confirmed, but once the correct space group was used, a number of interesting features of the structure emerged: (i) one third of the Al atoms are octahedrally coordinated (to four framework O atoms and two water molecules); (ii) the alternation of Al and P atoms is well defined; and (iii) there is a beautiful ordered water structure within the 18-ring channel. The octahedrally coordinated Al atoms are linked to one another *via* a hydrogen-bonded chain of water molecules which form a triple helix following the 6_3 axis in the channel. Furthermore, each chain of water molecules forms its own spiral as it follows the main helix (Fig. 10). This water structure, which has important implications in our understanding of the synthesis process, was an unexpected windfall from the Rietveld refinement. As an example of a Rietveld refinement profile plot, the observed, calculated and difference profiles for this refinement are shown in Fig. 11. The high crystallinity of the sample and the high resolution made possible by the use of synchrotron radiation combined to enhance the information content of the powder diffraction pattern. Even at high angles, sharp peaks with measurable intensity are observed. The R values for this refinement were $R_{wp} = 0{\cdot}141$, $R_F = 0{\cdot}086$ and $R_{\exp} = 0{\cdot}108$.

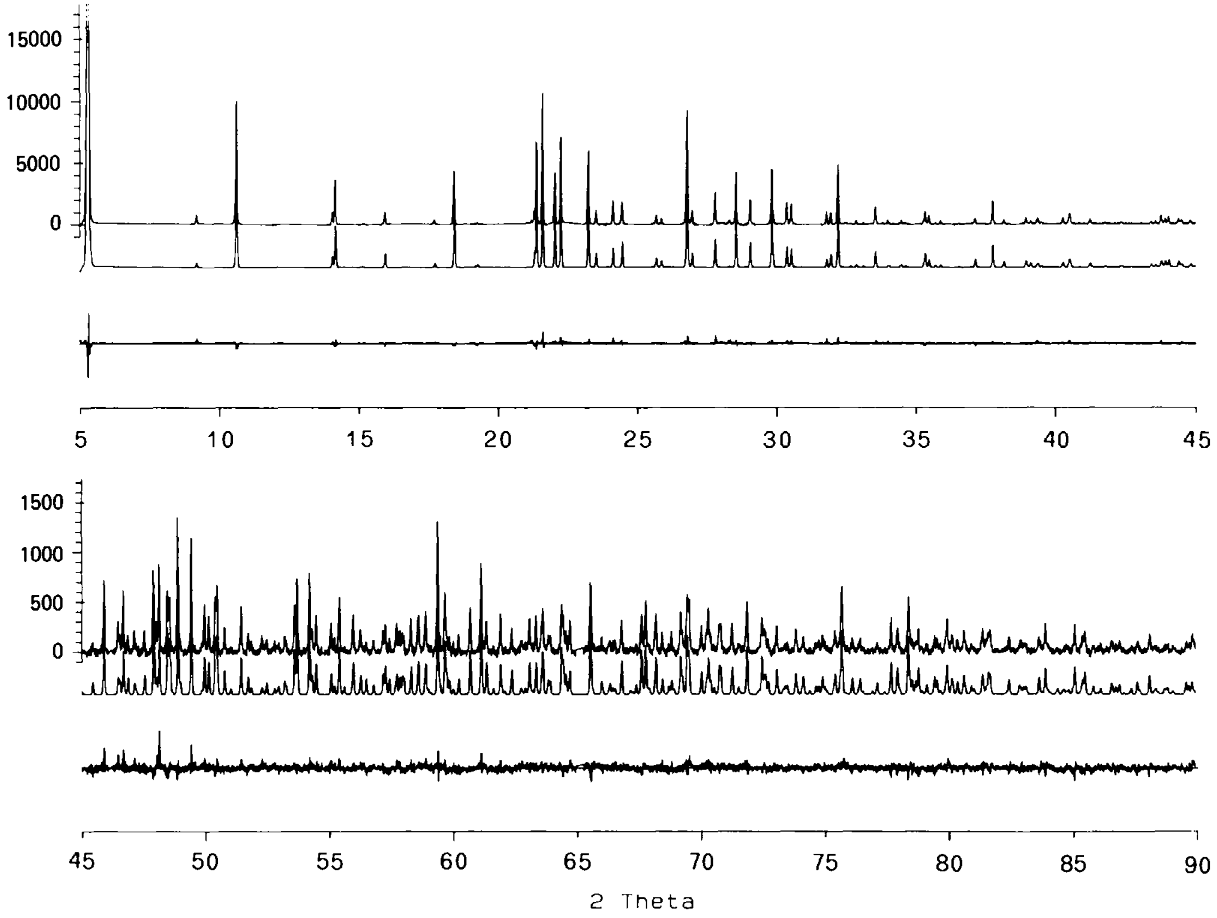

Fig. 11. The observed (upper), calculated (middle) and difference (bottom) profiles for the Rietveld refinement of as-synthesized VPI-5 (**VFI**). To show more detail, the first peak of the pattern has been cut at approximately 1/4 of its maximum intensity. For the same reason, the second half of the profile has been scaled up by a factor of eight.

Although it means digressing slightly from the central theme of framework structure determination, a short discussion of further applications of Rietveld refinement to zeolite structural science is perhaps appropriate at this point. The combination of Rietveld refinement and Fourier syntheses is a powerful one for the extraction of maximum structural information from a powder diffraction pattern. Once a framework topology is known and the space group for the material of interest has been determined, the location of extra-framework atoms, which is essential to the understanding of zeolite synthesis, ion exchange, sorption properties and catalytic activity, becomes possible.

In order to investigate the role of the organic material used in zeolite syntheses, two NU-3 (**LEV**) samples, one prepared in the presence of 1-aminoadamantane and the other in the presence of *N*-methylquinuclidinium iodide, were investigated (McCusker, 1989). Rietveld refinement and difference Fourier maps in the space group $R\bar{3}m$ showed the organic species to be located in very similar positions in the LEV cage (Fig. 12). The N atom of the 1-aminoadamantane is disordered over three positions because of the $\bar{3}$ axis, but the rest of the molecule follows the symmetry of the framework and is well ordered. Two orientations of the *N*-methylquinuclidinium ion (one with the methyl group pointing up and the other with it pointing down) were found in approximately equal proportions. The unit-cell parameters for the two materials reflect the differences in the shapes of the organic species. For the first sample, with the wider rounder 1-aminoadamantane 'template', $a = 13{\cdot}231$ and $c = 22{\cdot}290$ Å, whereas for the second sample, with the longer thinner *N*-methylquinuclidinium ion, $a = 13{\cdot}062$ and $c = 22{\cdot}601$ Å.

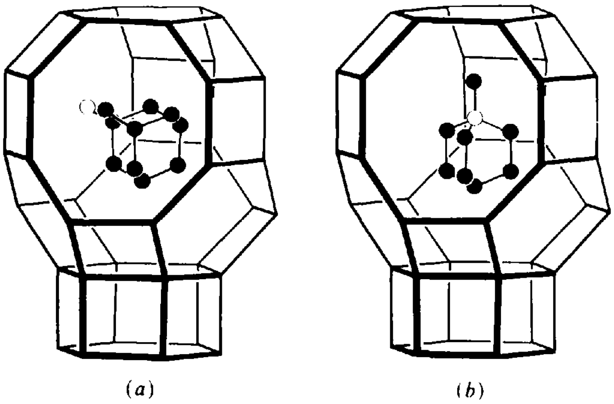

Fig. 12. The cage of the LEV structure type showing the location of (*a*) 1-aminoadamantane and (*b*) *N*-methylquinuclidinium in two different syntheses of NU-3. The filled circles are C atoms and the open ones N atoms. Only one orientation of each organic species is illustrated. Framework O atoms have been omitted for clarity.

To stabilize the early stages of refinement, to facilitate refinement of more complex zeolite structures, or to make refinement of unavoidably poor data possible (*e.g.* from a zeolite undergoing a transformation), geometric information in the form of expected bond distances and angles can be included as additional observations for the refinement (Waser, 1963; Hendrickson & Konnert, 1980; Baerlocher, 1982, 1991). This simultaneous DLS and Rietveld refinement of atomic coordinates has proven to be extremely useful in zeolite structure analysis, as long as care is taken in applying the restraints. For example, the mineral gobbinsite was thought to have the **GIS** framework topology, but the symmetry was ambiguous. Restrained refinement in several different orthorhombic space groups yielded good fits for the geometric observations in all cases, but in only one case was the fit to the X-ray data acceptable (McCusker, Baerlocher & Nawaz, 1985), and in this way the correct symmetry was established.

The final model must account for both the X-ray data and the geometric observations and, if incorrect assumptions are made in the application of the restraints, the X-ray data are unlikely to be well fitted. If heavy weighting of the geometric restraints is necessary to maintain reasonable framework geometry, it is an indication that the restraints are not compatible with the X-ray data and that the assumptions (*e.g.* the symmetry, the *T*-atom connectivity, the chemical identity of the *T* atoms or the coordination number of the *T* atoms) should be reconsidered. As long as these thoughts are kept in mind, restrained refinement smooths the progress of many zeolite structure analyses.

Rietveld refinement is an essential part of the framework structure determination process and has also been applied successfully to many zeolitic problems where the framework topology was already known. It is beyond the scope of this paper to go into too many details of those refinements. For further information the reader is referred to a review article entitled *Zeolite structure refinements using powder data* (Baerlocher, 1986).

Magic angle spinning NMR

Over the last ten years solid-state NMR in the field of zeolites has grown from a curiosity to a primary characterization technique. The sophistication of NMR instrumentation and methodology have increased dramatically in several directions pertinent to zeolite structural science. In contrast to diffraction experiments, which are sensitive to long-range order, NMR is sensitive to short-range effects and this makes it an extremely useful complementary technique. A brief overview of the NMR techniques pertinent to zeolite crystallography is given here, but for a more detailed and comprehensive treatment, the reader is referred to the book entitled *High-Resolution Solid-State NMR of Silicates and Zeolites* by Engelhardt & Michel (1987).

High-resolution ^{29}Si MAS NMR offers a wealth of structural information to zeolite crystallographers. For an aluminosilicate, the spectrum will show (to the first approximation) peaks (i) whose chemical shifts are correlated with the number of neighboring Al atoms the various Si atoms have and (ii) whose intensities reflect the proportion of the Si in the sample in such an environment. The absolute values of the chemical shifts are structure dependent, so care must be taken in the interpretation of spectra with less than the full complement of five peaks, corresponding to zero, one, two, three and four Al atoms in the second coordination shell. This information can be used to derive Si/Al ordering schemes, which are often difficult to detect with diffraction data.

For pure silicates, the ^{29}Si MAS NMR spectrum can be particularly informative. In the absence of the dominating effect of Al neighbors, the immediate chemical environment of the Si atoms becomes important and each crystallographically distinct Si site produces a slightly different chemical shift. Under the right conditions, then, the spectrum can reveal the number of Si sites in the asymmetric unit and their relative occupancies, and so some of the ambiguities regarding space-group choice can be eliminated. The assignment of peaks in a ^{29}Si NMR spectrum to specific sites in the zeolite framework structure is not straightforward, but it has been done now for a number of structures. Empirical correlations have been found between chemical shifts and structural parameters such as mean Si-O-T angles and Si-O bond lengths (Smith & Blackwell, 1983; Thomas, Kennedy, Ramdas, Hunter & Tennakoon, 1983; Ramdas & Klinowski, 1984). A theoretical basis for this observed correlation has also been advanced (Engelhardt & Radeglia, 1984).

A recent structure refinement of ZSM-11 (**MEL**) is a good example of how ^{29}Si NMR can be used to advantage in conjunction with powder diffraction (Fyfe, Gies, Kokotailo, Pasztor, Strobl & Cox, 1989). The authors were able to show by NMR that the postulated structure with seven T atoms in the asymmetric unit could only occur above room temperature ($\sim$333 K), since below that temperature more than seven peaks are observed in the ^{29}Si NMR spectrum. Structure refinement using data collected at 373 K progressed satisfactorily but, as might be expected, refinement of the same model using data collected at room temperature, where nine peaks are observed in the NMR spectrum, did not. The NMR spectrum was also able to show definitively that the sample was pure ZSM-11 with no ZSM-5 intergrowths.

Similarly, ^{29}Si NMR data on ZSM-12 (**MTW**) helped to elucidate the correct space group for refinement. The proposed structure in this case (LaPierre, Rohrman, Schlenker, Wood, Rubin & Rohrbaugh, 1985) proved to have the correct topology, but refinement of the structure using synchrotron powder diffraction data was successful only after the c-axis was doubled. The synchrotron data and Weissenberg photographs from a twinned crystal showed the doubling of the c axis to be necessary and the ^{29}Si NMR spectrum showed unambiguously which of two possible space groups ($C2/c$ and Cc with 7 and 14 T-atom positions, respectively) was the correct one (Fyfe, Gies, Kokotailo, Marler & Cox, 1990).

The recent application of two-dimensional solid-state ^{29}Si NMR to zeolitic systems is a very exciting development. The experiment can be used to observe ^{29}Si-O-^{29}Si interactions in the structure (*i.e.* the connectivity of the Si atoms in the framework) and can thus help tremendously in the evaluation of, or even in the generation of, new framework structures. Such experiments on a ^{29}Si-enriched sample of ZSM-39 (**MTN**) (Fyfe, Gies, Feng & Grondey, 1990) and on ZSM-12 (**MTW**) and KZ-2 (**TON**) with natural ^{29}Si abundance (Fyfe, Feng, Gies, Grondey & Kokotailo, 1990) have already demonstrated the feasibility and the tantalizing potential of this technique.

MAS NMR is not restricted to ^{29}Si. Both ^{31}P (nuclear spin 1/2) and ^{27}Al (nuclear spin 5/2) have been used extensively to investigate aluminophosphate molecular sieves. ^{31}P NMR is analogous to ^{29}Si NMR. The spectra are sensitive to the chemical environment of the P atoms in the framework structure and can give the number of P sites in the asymmetric unit and their relative occupancies. The chemical shifts can also indicate whether the neighboring Al atom is four, five or six coordinate, but, as with ^{29}Si NMR, care must be taken in the interpretation.

Until very recently, ^{27}Al NMR was limited more or less to the identification of the presence of tetrahedrally and/or octahedrally coordinated Al. This is primarily because the Al nucleus is quadrupolar and this leads to line broadening which obscures the isotropic chemical shift. As a result, only gross features of the spectrum could be observed. Fyfe *et al.* (1985) were able to improve the resolution of the ^{27}Al MAS NMR spectrum for zeolite omega (**MAZ**) by using a higher magnetic field and a higher rate of spinning. The spectrum showed two signals which were indicative of the presence of two non-equivalent tetrahedral Al sites.

Wu, Sun, Pines, Samoson & Lippmaa (1990) have now introduced a new 'double rotation' technique for obtaining high-resolution NMR spectra for half-odd-integer quadrupolar nuclei (*e.g.* ^{27}Al). The sample is placed in an inner rotor which itself is embedded in an outer rotor. The latter spins at the magic angle 54·74° with respect to the static magnetic field and the former at 30·56° with respect to the magic angle. The as-synthesized form of the very large-pore aluminophosphate VPI-5, which has 18-ring channels, was investigated using the technique and the spectrum showed three peaks indicative of two non-equivalent tetrahedral Al sites and one octahedral one with the relative site occupancies 1 : 1 : 1 (Wu, Chmelka, Pines, Davis, Grobet & Jacobs, 1990). As discussed in an earlier section, the Rietveld refinement of this material, which was done simultenously but independently of the NMR work, revealed that the previously assumed symmetry was too high and that there are in fact three Al sites, one of which is octahedral (McCusker, Baerlocher, Jahn & Bülow, 1991).

Microcrystal techniques

With the advent of synchrotron radiation as a viable source of high-intensity X-rays, single-crystal techniques can be applied to ever smaller crystals. The distinction between a powder and a single crystal has become a matter of definition. This, of course, has exciting implications in the field of zeolite science where so many samples are powders. Both white and monochromatic radiation techniques offer advantages to the zeolite crystallographer.

Laue diffraction methods have been developed considerably over the last few years (Helliwell *et al.*, 1989). The broad band of high-intensity X-rays provided by synchrotron-radiation sources has made Laue diffraction an attractive alternative to the slower monochromatic methods. Exposure times are a matter of seconds and the crystal is stationary. The potential for studying phase transitions or catalytic processes in zeolites *in situ* is obvious and promising. The scientists working in this area are primarily protein crystallographers, but at least one group has been investigating the feasibility of collecting and analyzing Laue diffraction data from very small inorganic crystals (Harding, Maginn, Campbell, Clifton & Machin, 1988; Rule, 1990). The range of 10 μm crystals has already been reached and smaller ones are being tested. In the case of most zeolites, the problem of anomalous dispersion is negligible, so the interpretation of the diffracted intensities, though time consuming, is fairly straightforward.

There is an interesting complementarity between Laue and powder diffraction data (Fig. 13). High-resolution powder data can usually be indexed without problems to give accurate lattice parameters, whereas normally only axial ratios can be calculated from Laue data. Given the unit-cell parameters, however, Laue data can be indexed and reflections with similar 2θ values do not overlap as they do in a powder pattern. Furthermore, intensities that can be extracted from a powder pattern with reasonable reliability usually lie near the center of reciprocal space (high *d* spacings), whereas those measured by Laue diffraction tend to lie further out at lower *d* spacings. Attempts to exploit this complementarity are in progress.

Another area in which the protein crystallographers have paved the way is in the use of area detectors for the collection of monochromatic diffraction data at synchrotron facilities. Again, the high intensity of the source makes data collection from very small crystals feasible. The crystal structures of two silicates, one the layer silicate EU-19 (Andrews *et al.*, 1988) and the other the zeolite theta-1 (**TON**) (Andrews, Papiz, Damas, Harding & Highcock, 1990), have been determined from such data collected at the SRS in Daresbury using an Enraf-Nonius FAST area detector. In both cases the crystals were very thin needles (8 × 18 × 175 and 4 × 18 × 125 μm, respectively). A feasibility study some years ago indicated that diffracted intensities from crystallites with volumes as small as 1 μm^3 could be measured with high precision (Eisenberger, Newsam, Leonowicz & Vaughan, 1984).

Concluding remarks

The increasing sophistication of the characterization techniques that can be applied to zeolitic systems allows ever more complex problems to be investigated. Model building is now based on more information (such as that provided by MAS NMR studies) than was previously available, the feasibility of applying direct methods to larger structures has increased with the advent of high-resolution powder diffraction and the application of single-crystal techniques to

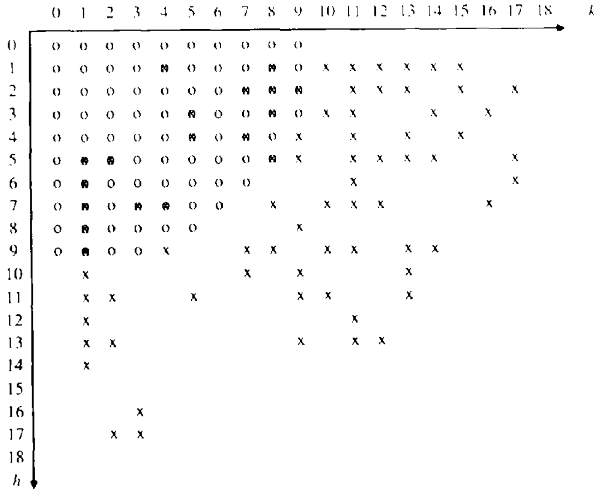

	0	1	2	3	4	5	6	7	8	9	10	11	12	13	14	15	16	17	18
0	O	O	O	O	O	O	O	O	O	O									
1	O	O	O	O	⊗	O	O	O	⊗	O	x	x	x	x	x	x			
2	O	O	O	O	O	O	O	⊗	⊗	⊗		x	x	x		x		x	
3	O	O	O	O	O	⊗	O	O	⊗	O	x	x			x		x		
4	O	O	O	O	O	⊗	O	⊗	O	x		x		x		x			
5	O	⊗	⊗	O	O	O	O	O	⊗	x		x	x	x	x			x	
6	O	⊗	O	O	O	O	O	O				x						x	
7	O	⊗	O	⊗	⊗	O	O		x		x	x	x				x		
8	O	⊗	O	O	O	O				x									
9	O	⊗	O	O	x			x	x		x	x		x	x				
10		x						x		x				x					
11		x	x			x				x	x			x					
12		x										x							
13		x	x							x		x	x						
14		x																	
15																			
16				x															
17			x	x															
18																			

Fig. 13. The *hk*0 layer of reciprocal space for the aluminophosphate phase kappa (structure unknown). The reflections for which intensity data could be extracted from a powder diffraction pattern (○) and from Laue diffraction data (×) are shown. Note the lack of axial reflection intensities from Laue data and the (sin θ)/λ limit for the powder data.

very small crystals has been made possible by the high intensity of synchrotron radiation.

Of the many structure-elucidation techniques now available to the zeolite crystallographer, no single one seems to dominate the field. Solving a new zeolite framework structure remains an art requiring patience, deductive reasoning and a proficiency in jigsaw-puzzle logic and is not guaranteed to succeed. However, for most of those working in the field, the result is well worth the effort and the frustrations encountered along the way. Not only is one assured that each structure determination and refinement signifies an advance in our understanding of zeolite science, but also that each new zeolite framework structure will be aesthetically pleasing.

I thank Professors W. M. Meier, H. Gies and R. M. Kirchner, Drs J. M. Bennett, M. M. Harding, G. Harvey and J. M. Newsam, and G. O. Brunner and M. Estermann for many useful discussions. I am also grateful to Professor C. Giacovazzo for sending me information prior to publication. Special thanks go to Dr Ch. Baerlocher, who not only contributed useful comments and suggestions regarding the manuscript, but also helped considerably in the production of the drawings. This work was supported in part by the Swiss National Science Foundation.

References

Andrews, S. J., Papiz, M. Z., Damas, A. M., Harding, M. M. & Highcock, R. M. (1990). *Acta Cryst.* C**46**, 172-173.

Andrews, S. J., Papiz, M. Z., McMeeking, R., Black, A. J., Lowe, B. M., Franklin, K. R., Helliwell, J. R. & Harding, M. M. (1988). *Acta Cryst.* B**44**, 73-77.

Arnold, H., Bartl, H., Fuess, H., Ihringer, J., Kosten, K., Löchner, U., Pennartz, P. U., Prandl, W. & Wroblewski, T. (1989). *Rev. Sci. Instrum.* **60**, 2380-2381.

Baerlocher, Ch. (1982). *XRS-82. The X-ray Rietveld System.* Institut fuer Kristallographie, ETH, Zurich, Switzerland.

Baerlocher, Ch. (1984). In *Proc. 6th Int. Zeolite Conf., Reno*, edited by D. Olson & A. Bisio, pp. 823-833. Guildford: Butterworths.

Baerlocher, Ch. (1986). *Zeolites*, **6**, 325-333.

Baerlocher, Ch. (1990). *EXTRACT. A Fortran Program for the Extraction of Integrated Intensities from a Powder Pattern.* Institut fuer Kristallographie, ETH, Zurich, Switzerland.

Baerlocher, Ch. (1991). In *Proc. IUCr Commission on Powder Diffraction, Rietveld Analysis Workshop, Petten, The Netherlands, June* 1989, edited by R. A. Young. Oxford Univ. Press.

Baerlocher, Ch., Hepp, A. & Meier, W. M. (1977). *DLS-76. A Fortran Program for the Simulation of Crystal Structures by Geometric Refinement.* Institut fuer Kristallographie, ETH, Zurich, Switzerland.

Baerlocher, Ch. & Meier, W. M. (1970). *Helv. Chim. Acta*, **53**, 1285-1293.

Baerlocher, Ch. & Meier, W. M. (1972). *Z. Kristallogr.* **135**, 339-354.

Ballmoos, R. von & Higgins, J. B. (1990). *Collection of Simulated XRD Powder Patterns for Zeolites. Zeolites*, Vol. **10**, pp. 313-529. (Special issue.) Stoneham, MA: Butterworth-Heinemann.

Bekkum, H. van, Flanigen, E. M. & Jansen, J. C. (1991). Editors. *Introduction to Zeolite Science and Practice. Studies in Surface Science and Catalysis*, Vol. 58. Amsterdam: Elsevier.

Bennett, J. M. (1988). *Am. Chem. Soc. Symp. Ser.* **368**, 162-176.

Bennett, J. M. & Gard, A. (1967). *Nature (London)*, **214**, 1005-1006.

Bennett, J. M. & Kirchner, R. M. (1990). Personal communication.

Bennett, J. M. & Kirchner, R. M. (1991). *Zeolites.* In the press.

Bialek, R. (1991). *KRIBER. A Pascal Program for the Generation of a DLS Input File.* Institut fuer Kristallographie, ETH, Zurich, Switzerland.

Breck, D. W. (1974). *Zeolite Molecular Sieves.* New York: Wiley.

Breck, D. W., Eversole, W. G., Milton, R. M., Reed, T. B. & Thomas, T. L. (1956). *J. Am. Chem. Soc.* **78**, 5963-5971.

Briscoe, N. A., Johnson, D. W., Shannon, M. D., Kokotailo, G. T. & McCusker, L. B. (1988). *Zeolites*, **8**, 74-76.

Brunner, G. O. (1990). *Zeolites*, **10**, 612-614.

Cartlidge, S., Wessicken, R. & Nissen, H.-U. (1983). *Phys. Chem. Miner.* **9**, 139-145.

Cascarano, G., Favia, L. & Giacovazzo, C. (1990). *SIRPOW. A Direct Methods Package Optimized for Powder Data.* Univ. di Bari, Italy.

Catlow, C. R. A. & Cormack, A. N. (1987). *Int. Rev. Phys. Chem.* **6**, 227-250.

Cox, D. E., Hastings, J. B., Cardoso, L. P. & Finger, L. W. (1986). *Mater. Sci. Forum*, **9**, 1-20.

Deem, M. W. & Newsam, J. M. (1989). *Nature (London)*, **342**, 260-262.

Delprato, F., Guth, J. L., Huve, L., Baron, J., Delmotte, L., Soulard, M., Anglerot, D. & Zivkov, C. (1989). In *Proc. 8th Int. Zeolite Conf., Recent Research Reports*, edited by J. C. Jansen, L. Moscou & M. F. M. Post, pp. 127-128. Amsterdam: Elsevier.

Eisenberger, P., Newsam, J. M., Leonowicz, M. E. & Vaughan, D. E. W. (1984). *Nature (London)*, **309**, 45-47.

Engelhardt, G. & Michel, D. (1987). *High-Resolution Solid-State NMR of Silicates and Zeolites.* Chichester: Wiley.

Engelhardt, G. & Radeglia, R. (1984). *Chem. Phys. Lett.* **108**, 271-274.

Flanigen, E. M., Bennett, J. M., Grose, R. W., Cohen, J. P., Patton, R. L., Kirchner, R. M. & Smith, J. V. (1978). *Nature (London)*, **217**, 512-516.

Fyfe, C. A., Feng, Y., Gies, H., Grondey, H. & Kokotailo, G. T. (1990). *J. Am. Chem. Soc.* **112**, 3264-3270.

Fyfe, C. A., Gies, H., Feng, Y. & Grondey, H. (1990). *Zeolites*, **10**, 278-282.

Fyfe, C. A., Gies, H. Kokotailo, G. T., Marler, B. & Cox, D. E. (1990). *J. Phys. Chem.* **94**, 3718-3721.

Fyfe, C. A., Gies, H., Kokotailo, G. T., Pasztor, C., Strobl, H. & Cox, D. E. (1989). *J. Am. Chem. Soc.* **111**, 2470-2474.

Fyfe, C. A., Gobbi, G. C., Kennedy, G. J., Graham, J. D., Ozubko, R. S., Murphy, W. J., Bothner-By, A., Dadok, J. & Chesnick, A. S. (1985). *Zeolites*, **5**, 179-183.

Gellens, L. R., Mortier, W. J. & Uytterhoeven, J. B. (1981). *Zeolites*, **1**, 11-18.

Gramlich, V. (1988). *Z. Kristallogr.* **182**, 100-102.

Gramlich, V. & Meier, W. M. (1971). *Z. Kristallogr.* **133**, 134-149.

Harding, M. M., Maginn, S. J., Campbell, J. W., Clifton, I. & Machin, P. (1988). *Acta Cryst.* B**44**, 142-146.

Helliwell, J. R., Habash, J., Cruickshank, D. W. J., Harding, M. M., Greenhough, T. J., Campbell, J. W., Clifton, I. J., Elder, M., Machin, P. A., Papiz, M. Z. & Zurek, S. (1989). *J. Appl. Cryst.* **22**, 483-497.

Hendrickson, W. A. & Konnert, J. H. (1980). In *Computing in Crystallography*, edited by R. Diamond, S. Ramaseshan & D. Venkatesan, pp. 13.02-13.23. Bangalore: Indian Academy of Sciences.

Higgins, J. B., LaPierre, R. B., Schlenker, J. L., Rohrman, A. C., Wood, J. D., Kerr, G. T. & Rohrbaugh, W. J. (1988). *Zeolites*, **8**, 446-452.

Highcock, R. M., Smith, G. W. & Wood, D. (1985). *Acta Cryst.* C**41**, 1391-1394.

Hill, R. J. & Gibbs, G. V. (1979). *Acta Cryst.* B**35**, 25-30.

Jacobs, P. A. & van Santen, R. A. (1989). Editors. *Zeolites: Facts, Figures, Future. Studies in Surface Science and Catalysis*, Vol. 49. Amsterdam: Elsevier.

Jansen, J., Peschar, R. & Schenk, H. (1990). *Acta Cryst.* A**46**, C57.

Katzer, J. R. & Gould, R. F. (1977). Editors. *Molecular Sieves-II. Am. Chem. Soc. Symp. Ser.* Vol. 40. Washington: American Chemical Society.

Kim, Y. & Seff, K. (1978). *J. Am. Chem. Soc.* **100**, 6989-6997.

Kokotailo, G. T., Lawton, S. L., Olson, D. H. & Meier, W. M. (1978). *Nature (London)*, **272**, 437-438.

Koningsveld, H. van, Jansen, J. C. & van Bekkum, H. (1987). *Zeolites*, **7**, 564-568.

Koningsveld, H. van, Jansen, J. C. & van Bekkum, H. (1990). *Zeolites*, **10**, 235-242.

Koningsveld, H. van, Tuinstra, F., van Bekkum, H. & Jansen, J. C. (1989). *Acta Cryst.* B**45**, 423-431.

LaPierre, R. B., Rohrman, A. C., Schlenker, J. L., Wood, J. D., Rubin, M. K. & Rohrbaugh, W. J. (1985). *Zeolites*, **5**, 346-348.

McCusker, L. B. (1988). *J. Appl. Cryst.* **21**, 305-310.

McCusker, L. B. (1989). In *Proc. 8th Int. Zeolite Conf., Recent Research Reports*, edited by J. C. Jansen, L. Moscou & M. F. M. Post, pp. 281-282. Amsterdam: Elsevier.

McCusker, L. B. & Baerlocher, Ch. (1984). In *Proc. 6th Int. Zeolite Conf., Reno*, edited by D. Olson & A. Bisio, pp. 812-822. Guildford: Butterworths.

McCusker, L. B., Baerlocher, Ch., Jahn, E. & Bülow, M. (1991). *Zeolites*. In the press.

McCusker, L. B., Baerlocher, Ch. & Nawaz, R. (1985). *Z. Kristallogr.* **171**, 281-289.

McCusker, L. B., Brunner, G. O. & Ojo, A. F. (1990). *Acta Cryst.* A**46**, C59.

Meier, W. M. & Olson, D. H. (1987). *Atlas of Zeolite Structure Types*. London: Butterworths.

Meier, W. M. & Uytterhoeven, J. B. (1973). Editors. *Molecular Sieves. Adv. Chem. Ser.* Vol. 121. Washington: American Chemical Society.

Meier, W. M. & Villiger, H. (1969). *Z. Kristallogr.* **129**, 411-423.

Mortier, W. J. (1982). *Compilation of Extra-Framework Sites in Zeolites*. London: Butterworths.

Murakami, Y., Iijima, A. & Ward, J. W. (1986). Editors. *New Developments in Zeolite Science & Technology. Proc. 7th Int. Zeolite Conf., Tokyo*. Amsterdam: Elsevier.

Newsam, J. M., Treacy, M. M. J., Koetsier, W. T. & de Gruyter, C. B. (1988). *Proc. R. Soc. London Ser.* A**420**, 375-405.

Norby, P., Christensen, A. N. & Andersen, I. G. K. (1986). *Acta Chem. Scand.* A**40**, 500-506.

Olson, D. & Bisio, A. (1984). Editors. *Proc. 6th Int. Zeolite Conf., Reno*. Guildford: Butterworths.

Olson, D. H., Kokotailo, G. T., Lawton, S. L. & Meier, W. M. (1981). *J. Phys. Chem.* **85**, 2238-2243.

Parise, J. B., Gier, T. E., Corbin, D. R. & Cox, D. E. (1984). *J. Phys. Chem.* **88**, 1635-1640.

Pattison, P., Cernik, R. J. & Clark, S. M. (1989). *Rev. Sci. Instrum.* **60**, 2376-2379.

Pauling, L. (1930*a*). *Proc. Natl Acad. Sci. USA*, **16**, 453-459.

Pauling, L. (1930*b*). *Z. Kristallogr.* **74**, 213-225.

Pawley, G. S. (1981). *J. Appl. Cryst.* **14**, 357-361.

Perego, G., Cesari, M. & Allegra, G. (1984). *J. Appl. Cryst.* **17**, 403-410.

Ramdas, S. & Klinowski, J. (1984). *Nature (London)*, **308**, 521-523.

Rees, L. V. C. (1980). Editor. *Proc. 5th Int. Conf. Zeolites, Naples*. London: Heyden.

Richardson, J. W. Jr, Smith, J. V. & Pluth, J. J. (1990). *J. Phys. Chem.* **94**, 3365-3367.

Riley, P. E. & Seff, K. (1975). *Inorg. Chem.* **14**, 714-721.

Rudolf, P. R., Saldarriaga-Molina, C. & Clearfield, A. (1986). *J. Phys. Chem.* **90**, 6122-6125.

Rule, R. J. (1990). PhD thesis, Univ. of Liverpool, England.

Seff, K. (1976). *Acc. Chem. Res.* **9**, 121-128.

Simmen, A., McCusker, L. B., Baerlocher, Ch. & Meier, W. M. (1991). *Zeolites*. In the press.

Smith, D. K., Nichols, M. C. & Zolensky, M. E. (1983). *POWD10. A Fortran IV Program for Calculating Powder Diffraction Patterns*-Version 10. University Park, PA, USA.

Smith, J. V. (1988). *Chem. Rev.* **88**, 149-182.

Smith, J. V. & Blackwell, C. S. (1983). *Nature (London)*, **303**, 223-225.

Taylor, W. H. (1930). *Z. Kristallogr.* **74**, 1-19.

Taylor, W. H. & Jackson, R. (1933). *Z. Kristallogr.* **86**, 53-64.

Taylor, W. H., Meek, C. A. & Jackson, W. W. (1933). *Z. Kristallogr.* **84**, 373-398.

Thomas, J. M., Kennedy, J., Ramdas, S., Hunter, B. K. & Tennakoon, D. T. B. (1983). *Chem. Phys. Lett.* **102**, 158-167.

Treacy, M. M. J., Newsam, J. M. & Deem, M. W. (1989). In *Proc. 8th Int. Zeolite Conf., Recent Research Reports*, edited by J. C. Jansen, L. Moscou & M. F. M. Post, pp. 285-286. Amsterdam: Elsevier.

Waser, J. (1963). *Acta Cryst.* **16**, 1091-1094.

Wu, Y., Chmelka, B. F., Pines, A., Davis, M. E., Grobet, P. J. & Jacobs, P. A. (1990). *Nature (London)*, **346**, 550-552.

Wu, Y., Sun, B. Q., Pines, A., Samoson, A. & Lippmaa, E. (1990). *J. Magn. Res.* **80**, 297-309.

Young, R. A. (1991). Editor. *Proc. IUCr Commission on Powder Diffraction, Rietveld Analysis Workshop, Petten, The Netherlands, June*, 1989. Oxford Univ. Press.

Yvon, K., Jeitschko, W. & Parthé, E. (1977). *J. Appl. Cryst.* **10**, 73-74.